Breeding and solitary wave behavior of dunes

O. Durán,[1] V. Schwämmle,[1,2] and H. Herrmann[1,3]
[1]*ICP, University of Stuttgart, 70569 Stuttgart, Germany*
[2]*Instituto de Física, Universidade Federal Fluminense, Av. Litorânea s/n, Boa Viagem; Niterói 24210-340, RJ, Brazil*
[3]*Departamento de Física, Universidade Federal do Ceará 60455-970 Fortaleza, Brazil*
(Received 17 June 2004; revised manuscript received 22 April 2005; published 31 August 2005)

Beautiful dune patterns can be found in deserts and along coasts due to the instability of a plain sheet of sand under the action of the wind. Barchan dunes are highly mobile aeolian dunes found in areas of low sand availability and unidirectional wind fields. Up to now modelization mainly focused on single dunes or dune patterns without regarding the mechanisms of dune interactions. We study the case when a small dune bumps into a bigger one. Recently Schwämmle and Herrmann [Nature (London) **426**, 610 (2003)] and Katsuki *et al.* [(e-print cond-mat 0403312)] have shown that under certain circumstances dunes can behave like solitary waves. This means that they can "cross" each other which has been questioned by many researchers before. In other cases we observe coalescence—i.e., both dunes merge into one—breeding—i.e., the creation of three baby dunes at the center and horns of a Barchan dune—or budding—i.e., the small dune, after "crossing" the big one, is unstable and splits into two new dunes.

DOI: 10.1103/PhysRevE.72.021308 PACS number(s): 45.70.Qj, 45.70.Vn, 89.20.−a

I. INTRODUCTION

We observe many different dune patterns in nature, such as, for example, longitudinal, transverse, star, and Barchan dunes. In regions where the wind blows mainly from the same direction sand availability determines the dune pattern. At high sand disposal transverse dunes dominate in the fields. They seem to be translationally invariant so that the lateral sand flux can be neglected. When less sand is available, Barchan dunes appear (Fig. 1). These are highly mobile, having the form of a crescent moon. Their velocity can reach up to several tenths of meters per year and is proportional to the reciprocal height, meaning that smaller dunes are faster than large ones. The surface of a Barchan dune can be divided into different sections: the windward side, the slip face after the brink, and the horns from which sand can leave the dune. Barchan dunes of different sizes are not perfectly shape invariant, and there exists a minimal height of 1–2 m below which they are not stable. These observations result from field measurements that have been made over the last decades [1–6]. Still many questions on dune dynamics remain open. Due to the large time scales involved in dune formation, full evolution of a dune is difficult to assess through measurements. Attempts have been made to get more insight through numerical calculations. Recently, several numerical models have been proposed in order to explain dune morphology and formation [7–20]. They have to deal with the calculation of the turbulent wind field, the saltation sand flux over the windward side, and the avalanches going down the slip face. Up to now modelization mainly focused on single dunes or dune patterns without regarding the mechanisms of dune interactions.

Recently, Besler found small Barchan dunes at the downwind side of big ones and concluded that Barchan dunes could behave like solitons [21,22]. This means that they would behave like solutions of nonlinear equations—for example, those describing waves in shallow water, which propagate through each other without changing their shape [23]. As an example see Fig. 1. In (a) and (b) a small Barchan dune is apparently ejected from the main dune, whereas in (c) small dunes emerge from the horns. Note the similarity with the snapshots of a collision simulation depicted in (d). Similar occurrences can be found in experiments with subaqueous Barchan dunes [28]. Nevertheless, most researchers believe that if a small Barchan dune hits a bigger one, it will be completely absorbed. This is motivated by the fact that a sand formation cannot cross the slip face of a dune without being destroyed. Therefore, the description of Barchan dunes as solitons has found very little support up to now, until Schwämmle *et al.* found that dunes can behave as solitary waves under certain conditions [24]. They show that, due to mass exchange, a big Barchan dune colliding with a smaller one placed behind may decrease its height until it becomes smaller, and therefore faster, than the previous one and leaves. Meanwhile, the initially smaller dune increases its height, becoming bigger and slower, in such a way that it looks as if the smaller dune crosses the big one. This situation was referred by analogy as solitary wave behavior despite the great differences with real water waves [25,26]. Katsuki *et al.* [27] also have obtained solitary wave behavior for coaxial and offset collisions of two subaqueous Barchan dunes.

In the following we use a minimal model for dunes to develop the morphological phase diagram for the coaxial collision between two Barchan dunes and show a possible size selection mechanism in Barchan fields.

II. MODEL

Our model [15,18,20] consists of three coupled equations of motion calculating the shear stress of the wind field, the sand flux, the avalanche flux, and the resulting change of the topography using mass conservation. The shear stress of the wind is obtained from the perturbation of the air flow over a smooth hill using the well-known logarithmic velocity pro-

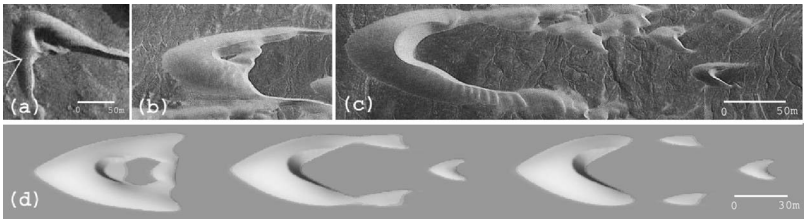

FIG. 1. Examples of the breeding process in two Barchan fields, Namibia (a) and Peru (b), (c), and in numerical simulations (d). The scale of the image in (b) and (c) is the same.

file of the atmospheric boundary layer. The shear velocity describes the strength of the wind. At the windward side of a Barchan dune the sand grains are transported by the so-called saltation mechanism [1]. Below, the big vortex of the wind field behind the brink the air cannot maintain sand transport. So the grains are deposited behind the brink in the lee zone of the Barchan dune until the surface reaches the angle of repose on which the sand flows down the slip face through avalanches.

The simulations are carried out with a completely unidirectional and constant wind source. In every iteration the horizontal shear stress $\boldsymbol{\tau}$ of the wind, the saltation flux $\mathbf{q}$, and the flux due to avalanches are calculated. The time scale of these processes is much shorter than the time scale of changes in the dune surface so that they are treated to be instantaneous. We perform all simulations using open boundary conditions with a constant influx. In the following the different steps at every iteration are explained.

a. The air shear stress τ on the ground. The shear stress is computed according to an analytical work describing the perturbation of the ground shear stress by a low hill or dune [29]. This perturbation is given by

$$\tilde{\hat{\tau}}_x = \frac{\tilde{h}_s k_x^2}{|\boldsymbol{k}|}\frac{2}{U^2(l)}\left\{-1+\left(2\ln\frac{l}{z_0}+\frac{|k|^2}{k_x^2}\right)\sigma\frac{K_1(2\sigma)}{K_0(2\sigma)}\right\},$$

$$\tilde{\hat{\tau}}_y = \frac{\tilde{h}_s k_x k_y}{|\boldsymbol{k}|}\frac{2}{U^2(l)}2\sqrt{2}\sigma K_1(2\sqrt{2}\sigma), \qquad (1)$$

where $\sigma=\sqrt{iLk_x z_0/l}$.

Here, K_0 and K_1 are modified Bessel functions. k_x and k_y are the components of the wave vector $\boldsymbol{k}$, the coordinates in Fourier space. $\tilde{\hat{\tau}}_x$ and $\tilde{\hat{\tau}}_y$ are the Fourier-transformed components of the shear stress perturbation in the wind direction and in the transverse direction. $\tilde{h}_s$ is the Fourier transform of the height profile, U is the vertical velocity profile which is suitably nondimensionalized, l the depth of the inner layer of the flow, and z_0 the roughness length which takes into account saltation. L is a typical length scale of the hill or dune and is given by a quarter of the mean wavelength of the Fourier representation of the height profile.

It has to be taken into account that the flow separates at the brink of the slip face of a dune. This is done by assuming an idealized "separation bubble," a region inside which there is no flow and outside of which the air flows as over a shape of the combined dune and bubble. Each slice in wind direction of the bubble is modeled by a third-order polynomial so that in the case of a Barchan dune the region between the horns is inside the bubble. The height profile h_s in Eqs. (1) is the profile of the dune including the separation bubble.

b. *The saltation flux q*. From the shear stress, the modification of the air flow due to the presence of saltating grains is accounted for. This results in an effective wind velocity driving the grains:

$$v_{\mathrm{eff}} = \frac{u_{*t}}{\kappa}\left\{\ln\frac{z_1}{z_0}+2\left[\sqrt{1+\frac{z_1}{z_m}\left(\frac{u_*^2}{u_{*t}^2}-1\right)}-1\right]\right\}, \qquad (2)$$

where $u_*=\sqrt{\tau/\rho_{\mathrm{air}}}$

The shear stress $\boldsymbol{\tau}$ results from Eqs. (1) through $\boldsymbol{\tau}=\boldsymbol{\tau}_0+|\boldsymbol{\tau}_0|\hat{\boldsymbol{\tau}}$, where $\boldsymbol{\tau}_0$ is the shear stress over a flat plane. z_0 is the roughness length of the sand excluding the effect of saltation, and $\kappa\approx 0.4$ is von Kármán's constant. z_m, the mean saltation height, and z_1 are parameters of the model.

The next step is the computation of the typical velocity of the saltating grains. It is determined by the balance between the drag force acting on the grains, the loss of momentum when they splash on the ground, and the downhill force. It is computed by solving the following quadratic vector equation numerically:

$$\frac{3}{4}C_d\frac{\rho_{\mathrm{air}}}{\rho_{\mathrm{quartz}}}d^{-1}(\mathbf{v}_{\mathrm{eff}}-\mathbf{u})|\mathbf{v}_{\mathrm{eff}}-\mathbf{u}|-\frac{g}{2\alpha}\frac{\mathbf{u}}{|\mathbf{u}|}-g\,\boldsymbol{\nabla}h=\mathbf{0}, \qquad (3)$$

where $\mathbf{v}_{\mathrm{eff}}=v_{\mathrm{eff}}\mathbf{u}_*/|\mathbf{u}_*|$. C_d is the drag coefficient of a grain. d_{grain} and ρ_{grain} are the diameter and the density of the grains. α is a model parameter.

The sand flux due to saltation is then obtained by numerically solving the transport equation

$$\mathrm{div}\,\mathbf{q}=\frac{1}{l_s}q\left(1-\frac{q}{q_s}\right)\begin{cases}\Theta(h), & q<q_s,\\ 1, & q\geqslant q_s,\end{cases} \qquad (4)$$

with

$$q_s=\frac{2\alpha}{g}|\mathbf{u}|(|\boldsymbol{\tau}|-\tau_t), \quad l_s=\frac{2\alpha|\mathbf{u}|^2}{\gamma g}\frac{\tau_t}{(|\boldsymbol{\tau}|-\tau_t)}. \qquad (5)$$

Here g is the gravity acceleration, and α, β, and γ are modal parameters taken from [30].

c. The time evolution of the surface. When the sand flux has been calculated, the height profile is updated according to the mass conservation

$$\frac{\partial h}{\partial t}=-\frac{1}{\rho_{\mathrm{sand}}}\mathrm{div}\,\mathbf{q}. \qquad (6)$$

d. Avalanches. In the last step, avalanches are simulated where necessary. If the slope of the sand surface exceeds the static angle of repose, sand is redistributed according to the sand flux:

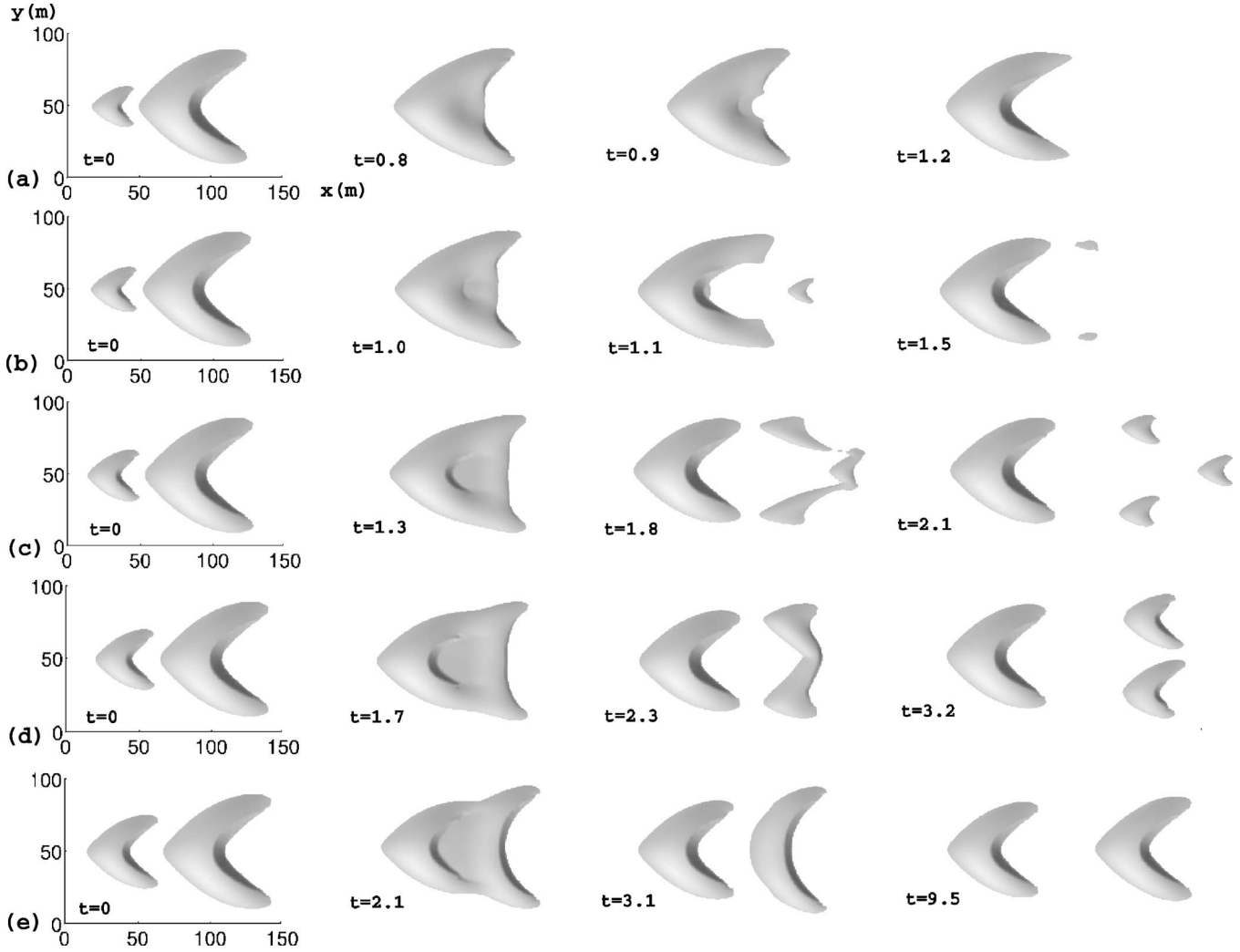

FIG. 2. Different situations during the collision of two Barchan dunes for $(V_h/V_H)_i$=0.06 (a), 0.08 (b), 0.12 (c), 0.17 (d), and 0.3 (e) using open boundary condition. Coalescence (a), breeding (b), (c), budding (d), and solitary wave behavior (e) take place. The time (t) is in month and the x and y labels in (a) are the same for all axes. The initial volume and height of the big Barchan dune is 6×10^3 m^3 and 5 m height, whereas the heights of the smaller Barchan are 1.8 m (a), 1.9 m (b), 2.2 m (c), 2.6 m (d), and 3.1 m (e).

$$\mathbf{q}_{\text{aval}} = E[\tanh|\nabla h| - \tanh(\tan\,\theta_{\text{dyn}})]\frac{\nabla h}{|\nabla h|}. \qquad (7)$$

The surface is repeatedly changed according to Eq. (6) using this flux, until the maximum slope is below the dynamic angle of repose, θ_{dyn}. The hyperbolic tangent function serves only to improve convergence.

All these steps are repeated iteratively to simulate the evolution of the shape.

III. RESULTS

We performed calculations by numerically solving the set of equations initially placing a big Barchan dune (volume V_H) downwind of a smaller one (volume V_h). The strength of the wind blowing into the system is fixed to a shear velocity of 0.5 m/s. The influx is 0.001 kg/ms, equal to the big Barchan equilibrium outflux. In order to take into account the lack of scale invariance of Barchan dunes, we repeat the simulations for two different sizes of the big Barchan dune, with initial volumes V_H: 6 and 70×10^3 m^3. The same general picture was observed. The smaller Barchan dune at some point bumps into the larger one. This leads to a hybrid state where the two dunes melt into a complex pattern. Four different situations can be observed: coalescence [Fig. 2(a)], breeding [Figs. 2(b) and 2(c)], budding [Fig. 2(d)], and solitary wave behavior [Fig. 2(e)] depending only on the relative sizes of the two dunes. Thus, we chose as control parameter the relative volume between the two dunes, V_h/V_H.

The evolution of the hybrid state can be understood as the result of a competition between two processes. The first one is the overlapping of both dunes at the beginning of the collision that eventually can lead to coalescence (Fig. 3, upper part). The second one is the effective mass exchange between the dunes due to the changes induced to the wind shear stress due to the approaching of both dunes. In the hybrid state the wind shear stress over the windward side of the bigger dune is reduced and, thus, crest erosion is enhanced. Besides, the wind shear stress over the lee side of the

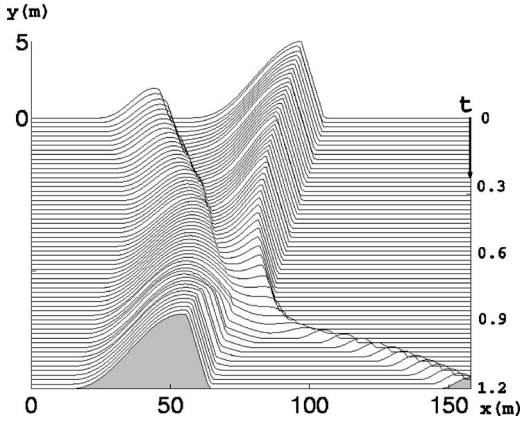

FIG. 3. Time evolution of the central slice of the "breeding" collision represented in Fig. 2(b). Note initially the small dune climbing on the bigger one and finally their mass exchange that leads to their separation. The time (t) is in months.

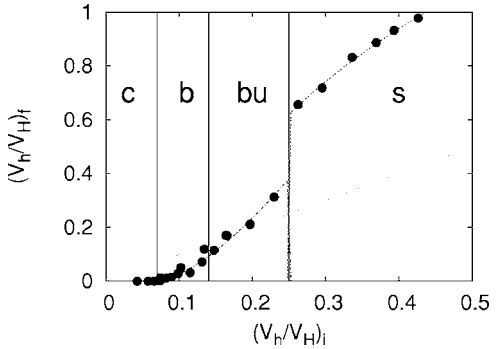

FIG. 4. Relation between the relative volume of the dunes before the collision $[(V_h/V_H)_i]$ and the relative volumes of the two largest dunes after the collision $[(V_h/V_H)_f]$. The regions in the morphological phase diagram are shown: coalescence (c), breeding (b), budding (bu), and solitary waves (s). For coalescence only one dune emerges and, thus, the relative volume is zero, whereas for solitary waves the relative volume strongly increases.

dune smaller is also reduced but enhancing crest deposition. Thus, the smaller dune may gain enough sand to become bigger than the one in front and therefore also become slower. In this way, the dune that was before the bigger one, can now become the smaller one and its velocity sufficiently large to leave the hybrid state. In this case the dunes separate again (Fig. 3, bottom).

The collision process is crucially affected by the separation bubble—i.e., the region after the brink and between the horns at which flow separation occurs (see item *a* in the Model section). After the separation at the brink, the flow streamlines reattach smoothly near the line segment whose end points are the horns. There, sand transport continues again. However, inside the separation bubble the flow is strongly reduced and, for simplicity, we set the flux to zero. Hence, the upwind dune will absorb that part of the downwind dune inside its separation bubble [Figs. 2(c)–2(e)].

For small relative volume ($V_h/V_H<0.07$) both dunes coalesce to a single one. In this case the relative velocity is high and hence the overlapping is faster than their mass exchange. Small dunes have a short slip face which disappears while climbing up the bigger one. This reduces the mass exchange and leads to a complete absorption of very small Barchan dunes [Fig. 2(a)]. For larger V_h/V_H the slip face survives for longer time, mass exchange becomes relevant, and a small Barchan dune is ejected from the central part of the dune (Fig. 3). The perturbation of the big dune shape, due to the overlapping of the small dune behind, also propagates over the horns since there is no slip face. At the end of each horn a small dune is ejected. This phenomenon of triple ejection we call "breeding." Figure 2(b) shows the snapshots. Note the qualitative similarity with the Barchan field shown in Fig. 1.

As the relative volume increases ($V_h/V_H>0.14$), a smaller relative velocity favors the mass exchange and reduces the overlapping process, leading to the complete separation of both dunes. Nevertheless, the dune leaving lacks the central part of its windward side and cannot reach the stable Barchan shape. Therefore, it splits into two new dunes, a phenomenon we call "budding" [Fig. 2(d)]. A similar phenomenon was reported in experiments with subaqueous Barchan dunes [28].

Between the "breeding" and "budding," a transition occurs at which the breeding three ejected dunes are connected forming a single dune that, afterwards, splits into three again [Fig. 2(c)]. For a higher relative volume the central ejected dune decreases its size until it disappears at budding. We consider this transition also as breeding.

When V_h/V_H is greater than 0.25, the instability of the dune in front disappears and both dunes develop to Barchan dunes. Then, we observe what we call solitary wave behavior as is shown in Fig. 2(e). In that case the dunes move with similar velocity and the mass exchange is the main process of the evolution of the hybrid state. The overlapping of both dunes is very small now and the emerging dune loses merely a small fraction of its tail. Effectively it looks as if the smaller dune just crosses the bigger one while in reality due to mass exchange the two heaps barely touch each other. The differences with real solitary waves was pointed out by Livingstone *et al.* [25] and discussed by Schwämmle *et al.* [26]. The analogy is based on the initial and final states of the colliding dunes, and not on the specific mechanism of interaction, which is very different as is shown in Fig. 3.

The morphological phase diagram crucially influences the evolution of the number of dunes in a Barchan field. In the coalescence region ($V_h/V_H<0.07$) the number of dunes decreases by 1, whereas three dunes in the breeding ($0.07<V_h/V_H<0.14$) and two dunes in the budding region ($0.14<V_h/V_H<0.25$) appear, and the number of dunes increases by 2 and 1 respectively. Finally, in the solitary wave region ($0.24<V_h/V_H$) a small dune seems to cross the bigger one and the number of them remains constant.

The collision process also change the volume distribution of the dunes in a Barchan field. Figure 4 shows the relative volume of the two largest dunes after the collision as a function of the relative volume of the initial ones. However, as their sizes are not constant in time, due to the permanent exchange of sand between the dunes and its intrinsic instability [17], we use the volumes of the dunes immediately

before and after they leave the hybrid state. As result of the interaction, the relative volume strongly increases after a solitary wave collision. In this case the collision process redistributes the initial mass, making both dunes more similar, giving rise to a size selection mechanism in Barchan fields [17]. Whereas for breeding and part of the budding collisions, although the number of small dunes that leave the hybrid state increases, they are smaller than the small dune before the collision.

Also it is interesting to note that the volume of the leaving dune in the breeding regime does not have a minimum value; thus, behind a Barchan dune it is possible to find small dunes of any height.

IV. CONCLUSIONS

In this work we develop a morphological phase diagram showing that during the collision of two Barchan dunes four situations can be observed: coalescence, breeding, budding, and solitary waves [Figs. 2(a)–2(e)]. At large scales the collision process depicted here could lead to a selection of a characteristic size of dunes in a Barchan field. However, we only considered perfectly aligned dunes.

Calculations of very large dune fields are still difficult because of high computational costs. One way out would be to consider a simplified model containing the main features of dune movement and interaction. For that purpose one could use the collision rules obtained in this work on a larger scale [31].

ACKNOWLEDGMENTS

We thank E. Parteli and A. O. Sousa for stimulating discussions and Max Plank Price and DAAD for financial support.

[1] R. A. Bagnold, *The Physics of Blown Sand and Desert Dunes* (Methuen, London, 1941).
[2] H. J. Finkel, J. Geol. **67**, 614 (1959).
[3] A. Coursin, Bulletin de l' I. F. A. N. **22A**, 989 (1964).
[4] P. A. Hesp and K. Hastings, Geomorphology **22**, 193 (1998).
[5] J. A. Jimenez, L. P. Maia, J. Serra, and J. Morais, Sedimentology **46**, 689 (1999).
[6] G. Sauermann, P. Rognon, A. Poliakov, and H. J. Herrmann, Geomorphology **36**, 47 (2000).
[7] F. K. Wippermann and G. Gross, Boundary-Layer Meteorol. **36**, 319 (1986).
[8] O. Zeman and N. O. Jensen, Risø National Lab. Report No. M-2738, 1988 (unpublished).
[9] P. F. Fisher and P. Galdies, Comput. Geosci. **14-2**, 229 (1988).
[10] J. M. T. Stam, Sedimentology **44**, 127 (1997).
[11] H. Nishimori, M. Yamasaki, and K. H. Andersen, Int. J. Mod. Phys. B **12**, 257 (1999).
[12] J. H. van Boxel, S. M. Arens, and P. M. van Dijk, Earth Surf. Processes Landforms **24**, 255 (1999).
[13] P. M. van Dijk, S. M. Arens, and J. H. van Boxel, Earth Surf. Processes Landforms **24**, 319 (1999).
[14] H. Momiji and A. Warren, Earth Surf. Processes Landforms **25**, 1069 (2000).
[15] K. Kroy, G. Sauermann, and H. J. Herrmann, Phys. Rev. Lett. **88**, 054301 (2002).
[16] B. Andreotti, P. Claudin, and S. Douady, Eur. Phys. J. B **28**, 315 (2002).
[17] P. Hersen *et al.*, Phys. Rev. E **69**, 011304 (2004).
[18] V. Schwämmle and H. Herrmann, Earth Surf. Processes Landforms **29**, 769 (2004).
[19] V. Schwämmle and H. Herrmann, Eur. Phys. J. E **16**, 57 (2005).
[20] G. Sauermann, K. Kroy, and H. J. Herrmann, Phys. Rev. E **64**, 031305 (2001).
[21] H. Besler, Phys. Bl. **10**, 983 (1997).
[22] H. Besler, Z. Geomorph. N. F. **126**, 59 (2002).
[23] G. L. Lamb, *Elements of Soliton Theory* (Wiley, New York, (1980).
[24] V. Schwämmle and H. Herrmann, Nature (London) **426**, 610 (2003).
[25] I. Livingstone, G. Wiggs, and M. Baddock, Earth Surf. Processes Landforms **30**, 255 (2005).
[26] V. Schwämmle and H. Herrmann, Earth Surf. Processes Landforms **30**, 517 (2005).
[27] A. Katsuki, H. Nishimori, N. Endo, and K. Taniguchi, J. Phys. Soc. Jpn. **24**, 538 (2005).
[28] N. Endo and K. Taniguchi, Geophys. Res. Lett. **34**, L12503 (2004).
[29] W. S. Weng *et al.*, Acta Mech. **2**, Suppl., 1 (1991).
[30] G. Sauermann, Ph.D. thesis, University of Stuttgart, 2001.
[31] A. R. Lima, G. Sauermann, K. Kroy, and H. J. Herrmann, Physica A **310**, 487 (2002).